World Scientific
www.worldscientific.com

An Improved Biologically-Inspired Image Fusion Method

Yuqing Wang

Key Laboratory of Airborne Optical Imaging and Measurement
Changchun Institute of Optics, Fine Mechanics and Physics
Chinese Academy of Sciences
No. 3888, Dong Nanhu Road, Changchun City
130033, Jilin Prov, P. R. China
wyq7903@163.com

Yong Wang

College of Communication Engineering
Jilin University, No. 5372, Nanhu Road
Changchun City, 130012 Jilin Prov, P. R. China

A biologically inspired image fusion mechanism is analyzed in this paper. A pseudo-color image fusion method is proposed based on the improvement of a traditional method. The proposed model describes the fusion process using several abstract definitions which correspond to the detailed behaviors of neurons. Firstly, the infrared image and visible image are respectively ON against enhanced and OFF against enhanced. Secondly, we feed back the enhanced visible images given by the ON-antagonism system to the active cells in the center-surrounding antagonism receptive field. The fused +VIS+IR signal are obtained by feeding back the OFF-enhanced infrared image to the corresponding surrounding-depressing neurons. Then we feed back the enhanced visible signal from OFF-antagonism system to the depressing cells in the center-surrounding antagonism receptive field. The ON-enhanced infrared image is taken as the input signal of the corresponding active cells in the neurons, then the cell response of infrared-enhance-visible is produced in the process, it is denoted as +IR+VIS. The three kinds of signal are considered as R, G and B components in the output composite image. Finally, some experiments are performed in order to evaluate the performance of the proposed method. The information entropy, average gradient and objective image fusion measure are used to assess the performance of the proposed method objectively. Some traditional digital signal processing-based fusion methods are also evaluated for comparison in the experiments. In this paper, the Quantitative assessment indices show that the proposed fusion model is superior to the classical Waxman's model, and some of its performance is better than the other image fusion methods.

Keywords: Image fusion; rattlesnake; retinex; human visual system.

1. Introduction

In the research area of sensor fusion, there are many technologies and algorithms. Their aim is to combine multiple input images into a single composite image which contains a better description of the scene than the one provided by any of the individual input images.[15] One of the most interesting characteristics of data fusion is its property of data aggregation. From the signal processing point of view, the process of data fusion extends spatial and temporal coverage of the system. Actually, information acquisition of human brain has close relation to the process of multi-sensor or multi-modal fusion. For example, human brain draws a conclusion from information from various perceptions, such as vision, touch and audition. In terms of the judgment of human brain, the final decision can be considered as composite judgment output from various sensors. In recent years, image fusion techniques have been deeply investigated. They now have wide applications in many fields, such as medical care, biological analysis and industry. In the field of image processing, the infrared and visible images are fused to obtain a composite image. The fused image contains visible targets and infrared targets. It is probable to find new form of target in the fused image. So, image fusion techniques are taken as an effective solution to improve the performance of recognition, target's detection and tracking. The quality of visual perception can also be improved by the dual band image fusion.[18]

Image fusion is not a process of simply combining multiple images. The quality of output image is increased by this process. It is the principal motivation of image fusion. Numerical algorithms in pixel-level fusion techniques may be classified as spatial domain and transform domain. In most of the algorithms, fusion mechanisms are developed by traditional signal processing methods, such as the sparse representation method,[2] Gaussian low-pass pyramid-based fusion method,[3] principal component analysis (PCA) method,[17] and the wavelet transform method.[5] In terms of these formalized processing systems, most of the state-of-the-art frameworks in image fusion are composed of some standardized methods. They are classified and shown in Fig. 1.

It can be seen from Fig. 1 that most of the current common image fusion methods need to go through four principal processes.[13]

Firstly, the imaging system needs to obtain source images. Then the spatial alignment is performed on the images. The dual band image fusion system captures visible and infrared images by dual band sensors. They describe the scene in visible band and infrared band. But the optical system gives different fields of view, the multiple images are kept aligned for image fusion.

Secondly, the aligned images need format transformation. The fusion system needs some kind of fixed image format which can be represented in the calculation framework, such as gray scale, color, quaternion and real number representation.

Thirdly, the image fusion is performed in the substantive stage. Many kinds of methods can be used in the process. Such as the pixel fusion, feature fusion and decision fusion.
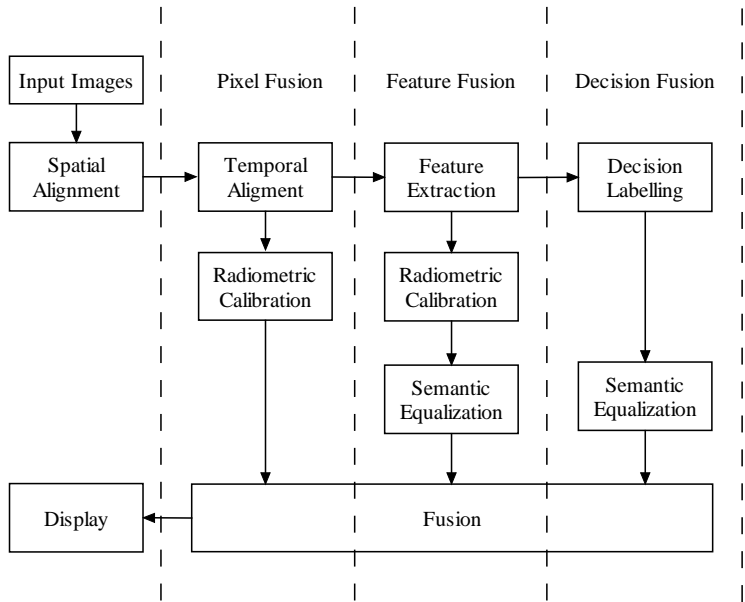
Fig. 1.   General image fusion framework in the imaging system.[13]

The fused image is shown in the final stage. The fused output is processed for display or further processing. In most of the studies, alignment is an independent part and it does not belong to the image fusion algorithms. It is assumed that image registration was performed in advance in these studies. In fact, the basic theories of traditional image fusion framework are from the common data fusion theory. It is considered as a migration process in the early studies. There is no significant HVS-inspired mechanism in the main process except some simple signal decomposition methods in the transform domain.

Another problem is that the real-time requirement can't be satisfied by the traditional fusion methods in most of the embedded systems. According to the principle of human visual system, thermal IR signals can't be detected by human eye, especially the long-wave infrared images.[4] So biologically-inspired image fusion method can scarcely be proposed by mimicking the mechanism of human visual system (HVS) which is occasionally used partly in source image preprocessing or information combination rather than the fusion mechanism. But in the research of Newman and Hartline,[14] the phenomenon of signal fusion was observed in several classes of rattlesnakes, such as pit vipers and pythons. The behaviors are actively investigated in their neurons of optic tectum. Similar to human visual system, visual perception of mammals is not performed pixel-by-pixel, it is performed by the global neuron control of brains subconsciously. Though the perception is performed by special sensor, purpose of the behaviors is as the same as those of many digital image processing methods, such as target detecting and tracking.[1,16,25]

In this paper, we begin the analysis using a biologically-inspired model. The fusion imaging system is analyzed theoretically from neuron interactions, signal transmission mechanisms and implementation methods. Previous work has revealed some useful information about biological fusion information reception behaviors. In the research of Waxman,[19–23] the mechanism of signal transmission and processing in the neuron system of rattlesnakes is described as a mathematical model. Neuron interactions in the brain are expressed as pixel interactions in an image in the studies of Waxman. But the model is simple and coarse due to the limited computational condition in the past. In this paper, we give an improved mathematical model to describe the complicated mechanism.

This paper is organized as follows: Section 2 discusses the mathematical representation of neuron interactions to representation of rattlesnake for the image fusion. In Sec. 3, a new fusion approach is proposed and analyzed. Some experimental results are presented in Sec. 4. Our conclusions and prospects are drawn in Sec. 5.

2. Image Fusion Mechanism of Rattlesnake

The biological model of rattlesnake visual system is the basis of our fusion algorithm. The computational approach is concluded from neurons' interactions in the optic tectum of rattlesnakes and pythons. The specific algorithm framework is inspired by the related work which has proven that the task is performed in a strongly nonlinear fashion.[22] The behaviors of rattlesnake visual system can be classified into enhancing behavior and depressing behavior. The interactions are shown by the neurons in which one sensing modality enhances or depresses another modality. Such as the interactions between infrared signal sensitive neurons and visible signal sensitive neurons. In fact, the reactions of the cells are related to their striking behaviors which are introduced in detail in Ref. 8.

The related work gives some physical motivations to our studies. The approaches are summarized by Waxman in Ref. 23. The work of Waxman is performed by constructing a mathematical model to simulate the interactions between these two kinds of cells. Experimental results show that the spectral reflectivity is linearly related to the emissivity. They also suggest the utility of ON and OFF response channels which form the basis of Waxman's computational model.[3] There are six kinds of behaviors in the interaction modes. The visible signal and output of IR receptive cell are defined as $f_{\mathrm{vis}}(x, y)$ and $f_{\mathrm{ir}}(x, y)$, respectively. These six kinds of behaviors are listed and introduced in what follows.

(1) The visible signals enhance IR signal receptive cells.

In this mode, the IR receptive cells don't respond to the individual visible signal input. But when the receptive cells are processing IR signals, the input visible signals can enhance the activities of neuron behaviors. We use the exponential function to simulate the enhancement procedure.

$$f_{\mathrm{vis+ir}}(x, y) = f_{\mathrm{ir}}(x, y) \exp f_v(x, y), \tag{1}$$

where $f_{\mathrm{vis+ir}}(x, y)$ denotes the output fused signal.

(2) The visible signals depress IR signal receptive cells.

It is contrary to the former mode. In this mode, the IR receptive cell doesn't respond to the individual visible signal input. But when the receptive cells are processing IR signals, the input of visible signals can depress the neuron behaviors. We use the logarithm function to simulate the depressing procedure.

$$f_{\mathrm{vis-ir}}(x, y) = f_{\mathrm{ir}}(x, y) \log[f_v(x, y) + 1], \tag{2}$$

where $f_{\mathrm{vis-ir}}(x, y)$ denotes the fused signal.

(3) The IR signals enhance visible signal receptive cells.

This mode is similar to mode (1). The difference is that the active signals are IR signals. They enhance or depress the visible signals. The visible signals are passive. We use the exponential function to simulate the process that IR signals enhance visible signals in this mode.

$$f_{\mathrm{ir+vis}}(x, y) = f_v(x, y) \exp f_{\mathrm{ir}}(x, y), \tag{3}$$

where $f_{\mathrm{ir+vis}}(x, y)$ denotes the fusion imagery.

(4) The IR signals depress visible signal receptive cells.

In this mode, the active IR signals act on the visible receptive cells by depressing their activities. We use logarithm function to simulate the depressing behaviors.

$$f_{\mathrm{ir-vis}}(x, y) = f_v(x, y) \log[f_{\mathrm{ir}}(x, y) + 1], \tag{4}$$

where $f_{\mathrm{ir-vis}}(x, y)$ denotes the fusion imagery.

(5) AND receptive cells.

In this mode, only when the visible signals and IR signals act on the receptive neurons simultaneously, the cells show obvious behaviors. We use "weighted-and" to simulate the corporation. It is defined as follows:

$$(a) \quad f_{\mathrm{and}}(x, y) = bf_v(x, y) + af_{ir}(x, y), \quad f_v(x, y) > f_{ir}(x, y), \tag{5}$$

$$(b) \quad f_{\mathrm{and}}(x, y) = af_v(x, y) + bf_{ir}(x, y), \quad f_v(x, y) < f_{ir}(x, y), \tag{6}$$

where $a > 0.5, b < 0.5$.

(6) OR receptive cells.

When the visible signals and IR signals act on the receptive neurons simultaneously or respectively, the cells show obvious behaviors. We use "weighted-or" to simulate the corporation. It is defined as follows:

$$(a) \quad f_{\mathrm{or}}(x, y) = af_v(x, y) + bf_{\mathrm{ir}}(x, y), \quad f_v(x, y) > f_{ir}(x, y), \tag{7}$$

$$(b) \quad f_{\mathrm{or}}(x, y) = bf_v(x, y) + af_{\mathrm{ir}}(x, y), \quad f_v(x, y) < f_{\mathrm{ir}}(x, y), \tag{8}$$

where $a > 0.5, b < 0.5$.

It is concluded from the research of visual system that the neurons in different locations in the retina show different reactions to illumination. The reactions are simplified to the behaviors of enhancing and depressing the visual system of

rattlesnake. In this paper, the region in the retina that can influence the reaction of neurons; receptive field is called RF. In many studies, the RF is considered as an elementary entity of nerve signal processing.[21]

According to the connections of retinal cone cell and visual cortex cell, the receptive field of neuron cells in retina can be divided into two parts: ON-center OFF-surround receptive field and OFF-center ON-surround receptive field.[3] They denote center enhancement behavior and surround depression behavior, respectively. We use two concentric circles composed of the ON-center receptive field and OFF-surround receptive field to describe the relation between two kinds of cells. The model is shown in Fig. 1, in which the plus sign denotes enhancement area and the minus sign denotes depression area. The enhancement area in the center and its surrounding depression area form the ON-center receptive field. When the beam strikes the center area, the neurons will be enhanced, but when the beam strikes its surrounding area, the neurons will be depressed. The activity of neurons in the ON-center area is weakened gradually from the center area to the surrounding area. But the OFF-surround receptive field shows the opposite behavior. Their different reactions in the central location and ambient location to the beam are named antagonism by biophysicists. These antagonism responses can be used to enhance the detail information of high frequency in the receptive image, then the image contour can be extracted by the behavior for further processing.

The biophysicists found that the region of the receptive field of ganglion cells near the retina are larger than that of the same kinds of cells far from the retina. The activities distribution of the cells in the central receptive field and surrounding receptive field complies with the Gaussian distribution. The sensitiveness of the cells near the central region of receptive field is higher than that in the receptive field far from the center.

In the study of E. H. Land in Refs. 9–11, the Retinex theory and approaches were proposed. The name comes from Retina and Cortex. The calculation of luminance and chrominance invariance was simplified to a calculable engineering model. Though the model is simple, it is highly related to the activities of cells in the receptive field. In the biological vision system, the ON-center receptive field and OFF-center receptive field play important roles in the processing of visual information in the cortex. The receptive field related model is used widely in the field of image processing.

The passive membrane equation is a mathematical description for center-surrounding antagonism receptive field model. It was proposed by Grossberg in his neural network description of center-surrounding receptive field.[6] The model is defined as follows:

Cell response of ON-antagonism system:

$$X_k(i,j) = \frac{AD + EC_k(i,j) - FS_k(i,j)}{A + C_k(i,j) + S_k(i,j)}.$$

(9)

Cell response of OFF-antagonism system:

$$\bar{X}_k(i,j) = \frac{AD + ES_k(i,j) - FC_k(i,j)}{A + C_k(i,j) + S_k(i,j)}, \tag{10}$$

where A denotes decay rate constant, i and j denote pixel coordinate, D denotes basal vitality of cells, and k is color channel. E and F are polarization constant. $C_k(i,j)$ denotes agitation center of receptive field, it is defined as:

$$C_k(i,j) = I_k(i,j) * W_c(i,j) = \frac{1}{2\pi\sigma_c^2} \sum_{m,n} I_k(i-m, j-n)e^{\left(-\frac{m2+n2}{2\sigma_c^2}\right)}.$$

$S_k(i,j)$ denotes depression-surrounding area in the receptive field, it is expressed as:

$$S_k(i,j) = I_k(i,j) * W_s(i,j) = \frac{1}{2\pi\sigma_s^2} \sum_{p,q} I_k(i-p, j-q)e^{\left(-\frac{p^2+q^2}{2\sigma_s^2}\right)},$$

where $I_k(i,j)$ is input image, "$*$" denotes convolution operator, $W_c(i,j)$ and $W_s(i,j)$ are Gaussian distribution functions corresponding to the central field and surrounding field. The size of their windows is denoted by $m \times n$ and $p \times q$. σ_c and σ_s are space constants corresponding to the central field c and surrounding field s.

3. Fusion Model

3.1. *Classical rattlesnake-inspired fusion model*

A classical rattlesnake-inspired fusion model was proposed by Waxman in Lincoln Laboratory of MIT. It is a pseudo-color fusion approach based on the dual-mode cell mechanism of rattlesnakes. The fusion process is shown in Figs. 2 and 3. The ON/ OFF framework represents the contrast perception properties. Enhancement is performed in the first stage. Then, the mechanisms of the infrared enhancing the visible and the infrared depressing the visible are performed in the second stage. They are consistent with the visual fusion mechanism of rattlesnake.

First, the infrared images are enhanced by the OFF-antagonism system and ON-antagonism system. Then the OFF-enhanced images and ON-enhanced images are obtained. The enhanced visible images are obtained by the ON-antagonism system.
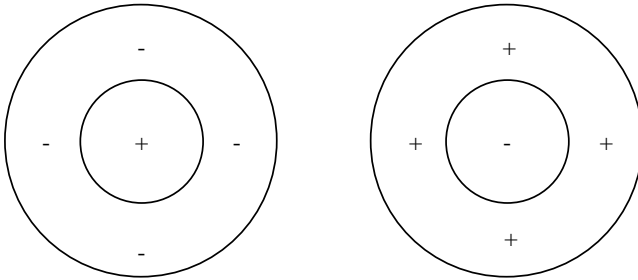
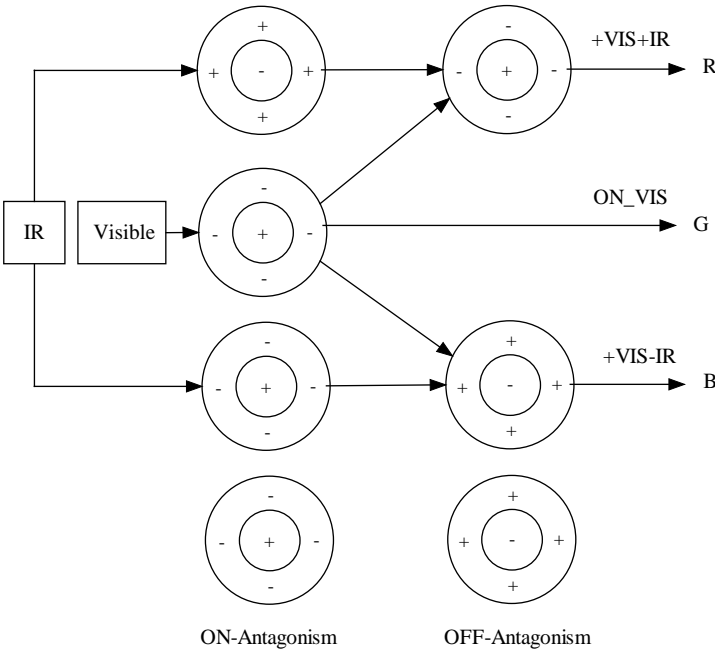Fig. 2.   Receptive fields of ON-center and OFF-center models.

Fig. 3.   Fusion model of Waxman.

It is expressed by ON_VIS in Fig. 2. Second, fusion is performed on the enhanced images. The neurons feedback the enhanced visible images from the ON-antagonism system to the cells in the center-surrounding antagonism receptive field. The OFF-enhanced infrared images and ON-enhanced infrared images are transferred to the surrounding-depressing cells in the corresponding neurons. Two types of fusion signals are acquired in the process. They are denoted as +VIS+IR and +VIS-IR which describe the infrared enhancing visible images and infrared depressing visible images. Finally, the three channels of R, G, B are constructed by the output signal of +VIS+IR, ON_VIS and +VIS-IR. Then the pseudo-color images are generated in the process.

3.2. *The proposed fusion framework*

Theoretically, the produced fused image by simulating the process of infrared image enhancing visible image and infrared image depressing visible image give a comprehensive description to the perceived information. In order to acquire more complicated information in the fused images, we improved the fusion framework of Waxman in Fig. 2. The fusion process is separated into two stages by simulating the fusion process of infrared and visible signals in the neurons of rattlesnakes. The proposed framework is shown in Fig. 4.
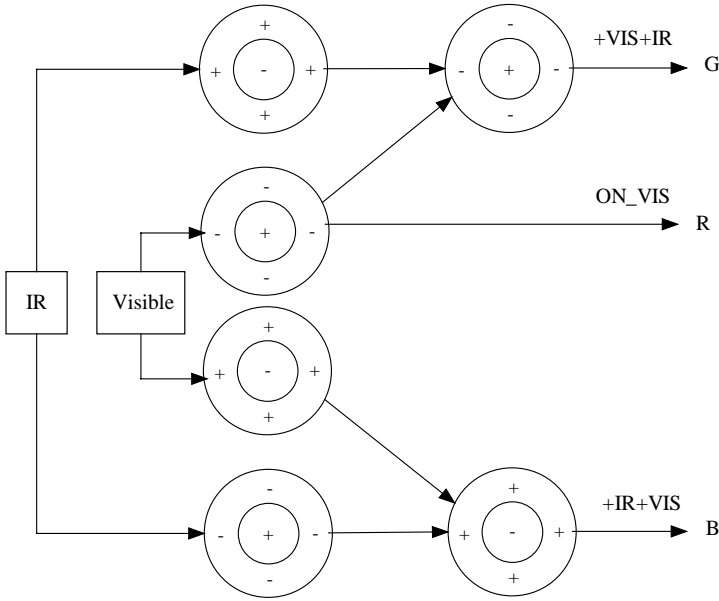
Fig. 4.   The proposed fusion framework.

In the new fusion method, the OFF- and ON-enhanced images are acquired in the first stage, the enhanced infrared image and visible image are also produced by the OFF-antagonism system and ON-antagonism system. Then the image fusion is performed in the second stage. We feed back the ON_VIS signal of the enhanced visible image from the ON-antagonism system to the active cells in the center-surrounding-antagonism receptive field. For the OFF-enhanced infrared image, we feedback them to the corresponding surrounding-depressing neurons in order to obtain the fused +VIS+IR signal. Then we feed back the enhanced visible signal from OFF-antagonism system to the depressing cells in the center-surrounded antagonism receptive field. The ON-enhanced infrared image is taken as input signal for the corresponding active cells in the neurons, then the cell response of infrared-enhancing-visible image is generated in the process, it is denoted as +IR+VIS. The three kinds of signals +VIS+IR, ON_VIS and +IR+VIS correspond to the RGB channels in the pseudo-color images. Then the output fused image is generated in the last step.

3.3. *Quality assessment methods of image fusion*

In order to further investigate the proposed model, we use three kinds of indices to assess the quality of fused images. The information entropy and average gradient are used to evaluate the active information in an image. The Qabf index is used to evaluate the amount of information transferred from source images to fused images.

(1) Information entropy

With respect to the total information contained in the fused image, there should be more information in the fused images than the source image. So the quality of fused images can be evaluated by the amount of the information entropy based on the assumption that the visual effect of fusion image with higher information entropy is better than that with lower information entropy.

$$H = -\sum_{i=0}^{L-1} p_i \log p_i, \tag{11}$$

where L is gray level of the pixel in the image, p_i is probability distributions of the pixel with different gray level.

(2) Average gradient

The amount of detail information in an image can be evaluated by computing its average gradient, which can describe the sharpness of the image. It is used to represent the difference between image details in the experiment. The index is defined as

$$\nabla \bar{G} = \frac{1}{M \times N} \sum_{i=1}^{M} \sum_{j=1}^{N} [\Delta x_f(i,j)^2 + \Delta y_f(i,j)^2]^{1/2}, \tag{12}$$

where $M \times N$ denotes the size of fused image. $\Delta x_f(i,j)$ is gradient in the x direction of pixel (i,j). $\Delta y_f(i,j)$ expresses the gradient in the y direction of pixel (i,j).

(3) Objective Image Fusion Performance Measure

The above two metrics assess the quality of fused images by calculating the activities of their pixel distribution. In fact, the statistical results give a description for the amount of energy included in an image. But it is not a comprehensive mechanism to evaluate image quality. The HVS-sensitive information in an image is the information that the metrics should assess.[7,12] The objective image performance measure in Ref. 24 is more reasonable because it can evaluate the quality of fused images by calculating the amount of edge information that is transferred from the input images to the fused images. The mechanism is consistent with the properties of HVS. The metric is named Q_{abf}, and it is defined as follows:

$$Q_{abf} = \frac{\sum_{n=1}^{N} \sum_{m=1}^{M} Q^{AF}(n,m)\omega^A(n,m) + Q^{BF}(n,m)\omega^B(n,m)}{\sum_{i=1}^{N} \sum_{j=1}^{M} (\omega^A(i,j) + \omega^B(i,j))}, \tag{13}$$

where Q^{AF} and Q^{BF} are edge information preservation values which are weighted by $\omega^A(n,m)$ and $\omega^B(n,m)$, respectively. A Sobel edge operator is applied in the operators.[24]

4. Experimental Results

In the experiments, two sets of OCTEC test images are firstly used to simulate the proposed method. Image registration was performed on the produced source images in advance. They are shown in Fig. 5, where Figs. 5(a) and 5(c) are visible images and Figs. 5(b) and 5(d) are corresponding long wave infrared images. The source images

Fig. 5.   Source images from OCTEC.

Figs. 5(c) and 5(d) are photographed in the smoke environment in order to emphasize the effect of infrared imagery.

In order to give a comprehensive investigation on the improved biologically inspired image fusion mechanism, we use some traditional fusion methods to test the images for comparison. The results are given in Fig. 6.

Theoretically, in respect of the human visual system, the pseudo-color images show very different visual effects in Fig. 6. They are not very consistent with the
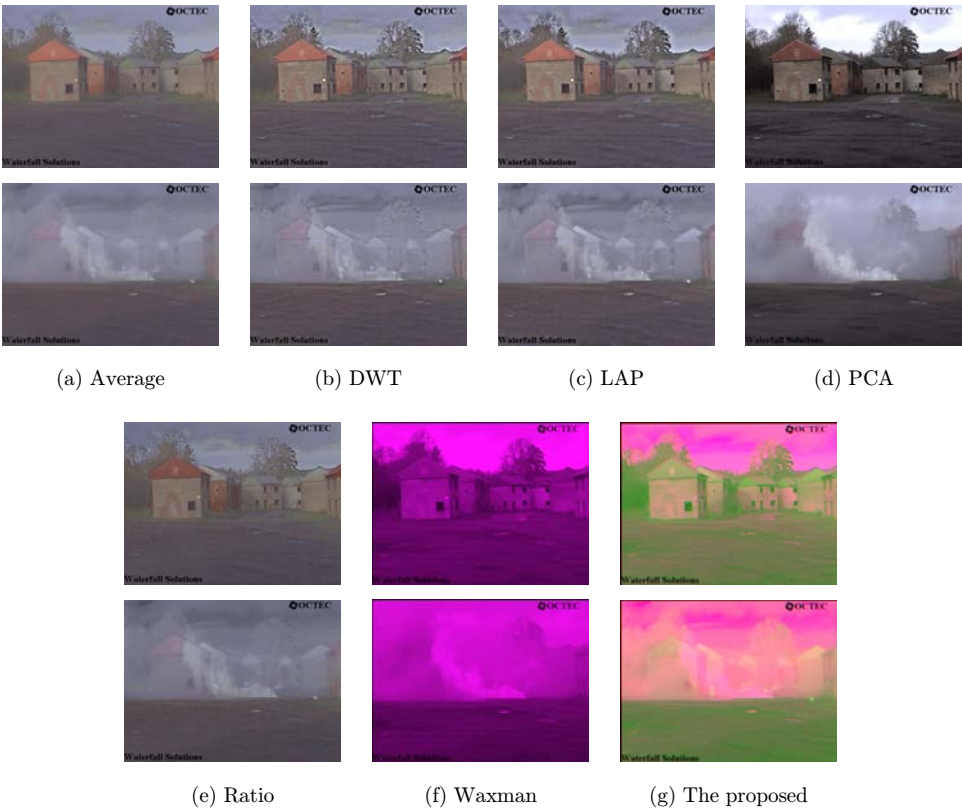

(a) Average   (b) DWT   (c) LAP   (d) PCA

(e) Ratio   (f) Waxman   (g) The proposed

Fig. 6.   Color image fusion results.

(a) Average (b) DWT (c) LAP (d) PCA

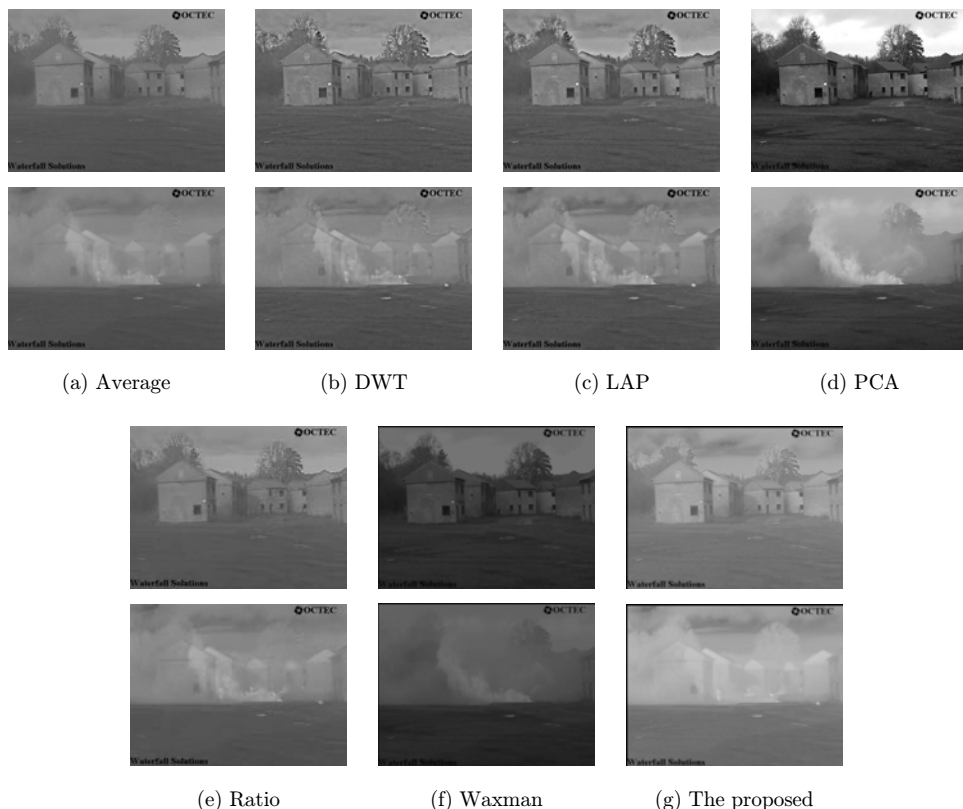(e) Ratio (f) Waxman (g) The proposed

Fig. 7. Grayscale image fusion results.

properties of human perception. But in most of the applications, we did not pay much attention to the color information. Main structure information in an image is described by the pseudo-color information. In order to further investigate the performance of the proposed method, we transform the color images in Fig. 6 to grayscale images. They are shown in Fig. 7.

From the fusion results in Figs. 6 and 7, it can be clearly seen that the fusion results of the proposed methods are better than the results of Waxman. The perceived effect of Fig. 7(g) is close to the natural scene. Some visible objects are more prominent. The detail information in the scene is also better than that from the classical fusion method of Waxman. The smoke shelter houses, people and the fire point can hardly be seen in Waxman's results in Figs. 6 and 7. Figures 6(g) and 7(g) are fusion results obtained by using the fusion structure proposed in this paper. It not only preserves the background information of visible light images such as houses, trees, people and smoke but also contains the main information in the infrared image such as thermal target and heat source location. It should be pointed out that compared with the complicated DWT-based method, the proposed biologically-inspired image fusion method does not show performance improvement obviously in

the grayscale image fusion results in Fig. 7. But in Fig. 6, the pseudo color fused images generated by the proposed method show better perceptive quality. There is abundant information in these fused images which show stronger contrast than the other fused images. The visual impact of Fig. 6(g) is also stronger than other fused images. The fused images of Fig. 6(f) given by Waxman are also pseudo color images, but their visual effect is similar to the fused image of Fig. 6(d) using PCA method. The color contrast is almost the same as in the source visible image. There is no information increase in these fused images. Quantified index is an effective objective tool to evaluate image quality. It can give precise assessment result for test images. We use information entropy, average gradient and objective image fusion performance measure to assess the quality of image fusion. For each index, the luminance layer of these fused images and the three R G B channels are all assessed by the quantified index. Regarding the color information, transferring is only performed in Waxman's method and the proposed method. The color information is not used in the assessment. We compute the average value of the R G B layers of the pseudo color images. The results are listed in Table 1.

Seven fusion methods are used for comparisons in the experiments. They are average method, wavelet-based method, Laplace pyramid method, PCA method, ratio pyramid method, the Waxman's method and the proposed method. In general, the performance of the wavelet-based method should be the best among them. According to the objective assessment results listed in Table 1, the PCA-based method achieves the best performance in the fusion methods. But it almost does not implement the fusion task in the process. It can be seen clearly that the method does not transfer useful information from source image to the fused image. Considering the visual perception effect and objective assessment results, the wavelet-based method, Laplace pyramid method and the proposed method give better performance than the other methods. The performance differences between the three methods lies

Table 1.   Assessment results of fused images in Figs. 6 and 7.

| Index		Average	DWT	LAP	PCA	Waxman	Ratio	Proposed
Fused images of Figs. 5(a) and 5(b)								
Information entropy	Luminance only	6.3162	6.5683	6.6110	7.0633	5.8477	6.5031	6.1623
	All information	2.1054	2.1894	2.2037	2.3544	5.8411	2.1677	6.5136
Mean gradient	Luminance only	0.0194	0.0306	0.0304	0.0357	0.0078	0.0235	0.0119
	All information	0.0065	0.0306	0.0101	0.0119	0.0116	0.0078	0.0187
Qabf	Luminance only	0.4499	0.6257	0.6536	0.6783	0.0492	0.4517	0.0780
	All information	0.1500	0.2086	0.2179	0.2261	0.0733	0.1506	0.0911
Fused images of Figs. 5(c) and 5(d)								
Information entropy	Luminance only	6.1211	6.2656	6.3063	6.9289	5.9428	6.2383	6.4239
	All information	2.0404	2.0885	2.1021	2.3096	5.8858	2.0794	6.7725
Mean gradient	Luminance only	0.0136	0.0181	0.0177	0.0166	0.0062	0.0155	0.0110
	All information	0.0045	0.0060	0.0059	0.0055	0.0094	0.0052	0.0103
Qabf	Luminance only	0.4394	0.4811	0.5093	0.6149	0.0515	0.4554	0.0944
	All information	0.1465	0.1604	0.1698	0.2050	0.0866	0.1518	0.1025

| (a) | (b) | (c) | (d) |
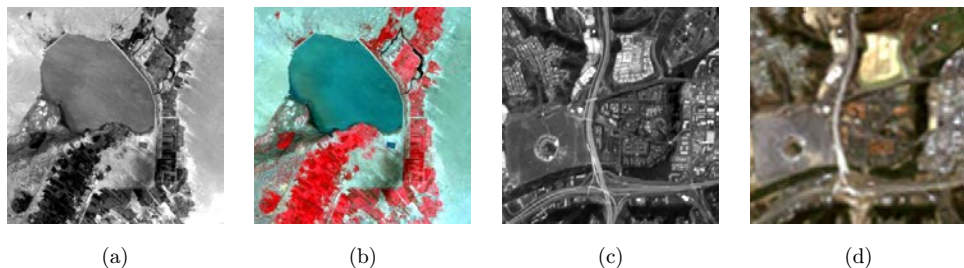
Fig. 8.   Remote sensing source images.

is their description of the detail information in an image. The detail information distribution in the luminance layer of fused images using wavelet-based method and Laplace pyramid method is more abundant than the proposed method. But the color contrast of the fused images generated by the proposed method is better than the fused image produced by wavelet-based method and Laplace pyramid method. Behaviors of these methods are deeply investigated by another group of images. They are shown in Fig. 8. The corresponding experimental results are shown in Fig. 9.

Though the proposed method is inspired by the mechanism of visible and infrared fusion process, it can be expanded to the general image fusion applications. Figure 8 gives two groups of remote sensing images. There are also grayscale images and color images in the data set. From the experimental results in Fig. 9, we can see that the behaviors of these fusion methods are similar to those in Figs. 6 and 7. The proposed method improves the contrast of the fused images. But the detail information in Fig. 9(g) is not as good as the wavelet-based method and Laplace pyramid method. Their quantified assessment results are given in Table 2, we perform the same assessment method in Table 1.

Due to the disadvantages of detail information expression, the proposed method gives lower value of Qabf than most of the traditional fusion methods, but it is higher than the Waxman's method. For some source images, it is better than the average method and PCA method. In the evaluation with Information entropy and Mean gradient of all information it is better than the other methods, because the proposed method transfers all the information to the fused images. But the traditional methods only transfer the luminance information to the fused images. The detail behaviors of the proposed method is investigated by the local image analysis. The test images are shown in Fig. 10.

The detailed description by the proposed method of the image is analyzed by enlarging its local region. In Fig. 10, the local region at the same place of four fused images are enlarged two times in order to give a clear visual effect of their local behaviors. Because the rightmost images are enlarged too much to show their contours, we list the number of grayscale or color in the enlarged images for comparing in Table 3.

Obviously, five kinds of regions with different color in the enlarged local images are distinguished by the proposed method. It shows that the proposed method can describe the local information better than the other fusion methods. But because the image contour is usually extracted in luminance layer and the converting from color image to grayscale image results in the loss of information in the grayscale images, the visual perception of the contour information in the luminance layer of the fused images generated by the proposed method is not as good as those generated by the wavelet-based method and pyramid method. It can be seen clearly in Figs. 8 and 9. The objective assessment methods give similar results in Tables 1 and 2.

From the objective assessment results of Information entropy, Mean gradient and Qabf indices, we can see that the proposed biologically-inspired method gives similar results to the source images compared with the complicated wavelet-based method. In general, fusion images generated by better fusion methods should contain more
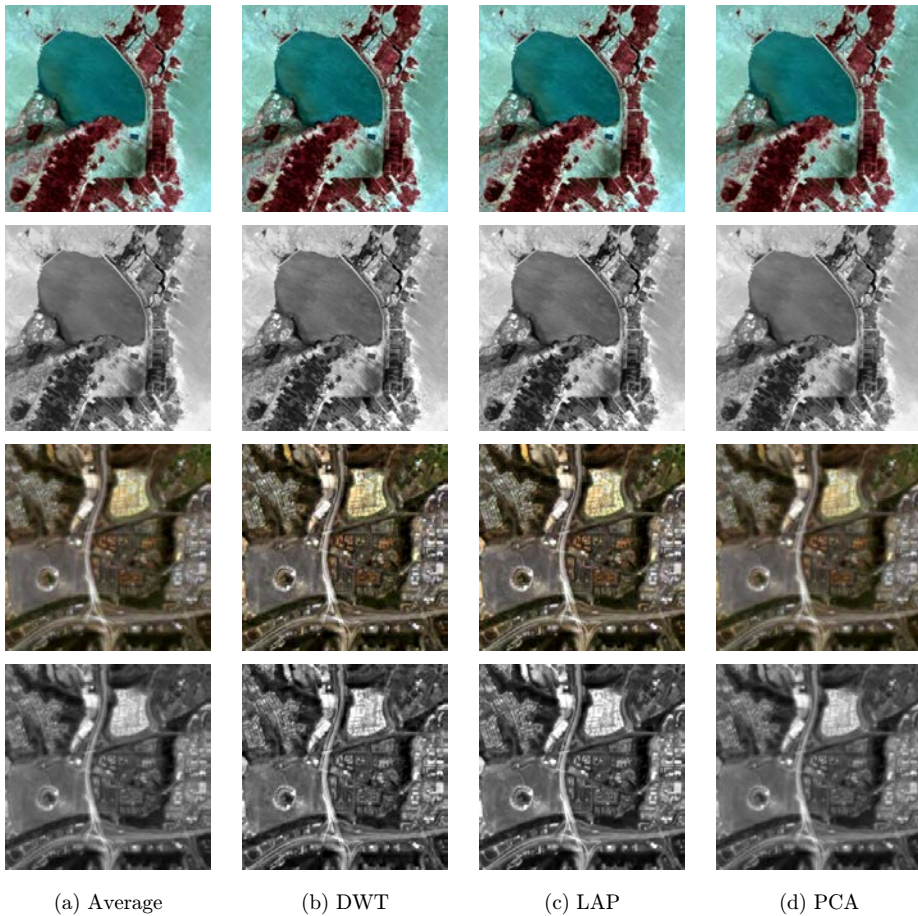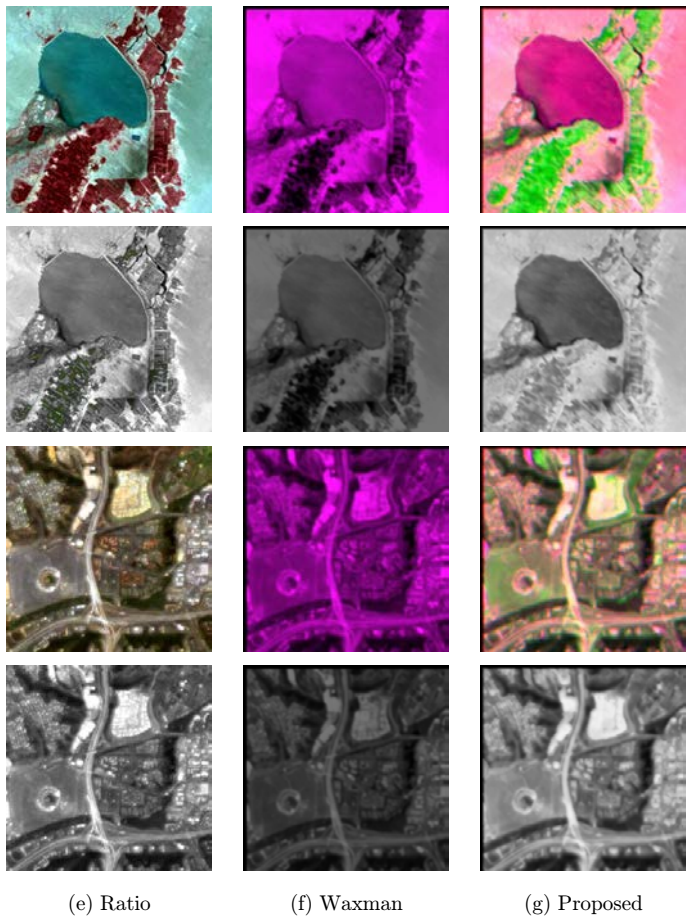

(a) Average   (b) DWT   (c) LAP   (d) PCA

Fig. 9.   Fused images of Fig. 8.

(e) Ratio   (f) Waxman   (g) Proposed

Fig. 9.   (*Continued*)

Table 2.   Assessment results of fused images in Fig. 9.

| Index		Average	DWT	LAP	PCA	Waxman	Ratio	Proposed
Fused images of Figs. 8(a) and 8(b)								
Information entropy	Luminance only	7.6523	7.7141	7.7453	7.6709	6.6217	7.5754	7.1445
	All information	2.5508	2.5714	2.5818	2.5570	6.4466	2.5251	6.8348
Mean gradient	Luminance only	0.0719	0.0869	0.0859	0.0729	0.0235	0.0836	0.0389
	All information	0.0240	0.0290	0.0286	0.0243	0.0384	0.0279	0.0586
Qabf	Luminance only	0.8318	0.7939	0.8156	0.8344	0.0558	0.7750	0.1025
	All information	0.2773	0.2646	0.2719	0.2781	0.0784	0.2583	0.1110
Fused images of Figs. 8(c) and 8(d)								
Information entropy	Luminance only	7.3751	7.5362	7.5820	7.3761	6.4741	7.5967	7.5272
	All information	2.4584	2.5121	2.5273	2.4587	6.2921	2.5322	7.4003
Mean gradient	Luminance only	0.0576	0.0962	0.0954	0.0568	0.0266	0.0770	0.0498
	All information	0.0192	0.0321	0.0318	0.0189	0.0435	0.0257	0.0680
Qabf	Luminance only	0.4421	0.5447	0.5729	0.4348	0.0627	0.4860	0.1181
	All information	0.1474	0.1816	0.1910	0.1449	0.0742	0.1620	0.1158
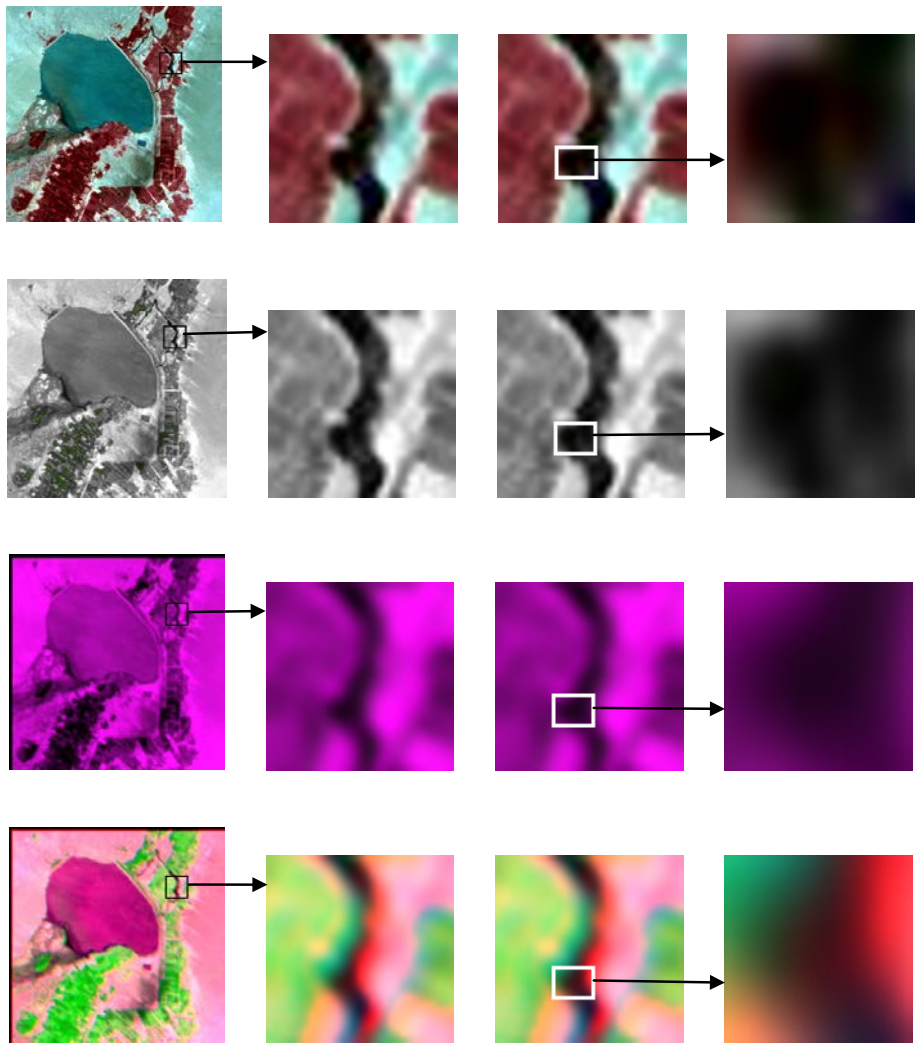
Fig. 10. Local image analysis.

Table 3. Number of grayscale or color in the enlarged images of Fig. 10.

Enlarged Images	Laplace Pyramid (Color)	Laplace Pyramid (Grayscale)	Waxman's Method	The Proposed
Number of Grayscale or color	3	3	2	5

detail information, so they have greater information entropy and average gradient
than other methods. But by analyzing the local images of the fused images, we find
that application of this assessment criterion should be restricted in the grayscale
images. Color contrast of the proposed method is better than in the other methods,

though its fused images do not establish an obvious superiority in the detail information description in luminance layer. Even so, it can be seen from the experimental results that for both sets of grayscale and color images, the information entropy and mean gradient of this method are better than those of the classical method of Waxman. Drawback of the proposed method is the time consuming calculating process. Our experimental results also show that the simulation time of the proposed algorithm is longer than that of Waxman's algorithm and other fusion methods. Since we didn't implement any optimization on the proposed algorithm, it needs further improvement to reduce image fusion time.

5. Conclusions

In summary, both from the visual perception and quantitative evaluation results, the experiments of the proposed method give a feasible algorithm structure to fuse dual-band images by simulating the visual system of rattlesnakes. The experimental results show that the imaging process is well consistent with the behaviors of predatory rattlesnakes. Properties of the proposed method can be summarized in two points.

(a) The fused images present strong color contrast in global and local information distribution. Image content is described by color information. It is different from the traditional methods which is based on calculating pixel distribution of luminance layer.

(b) The color information is transferred from the source images to the fused images. So, the fusion process is implemented by full information transmission.

The predatory behavior of rattlesnakes is accurate and reliable. Their processing mechanism which is dominated by the neurons should satisfy the condition of real-time and celerity. So, there cannot be complicated signal decomposition in the process. In this paper, as the discussion above, we are concerned for not only the visual system simulation of rattlesnake but also its applications in image processing. We proposed a very simple model to simulate the behaviors of rattlesnake. It is easy to implement but gives a common fusion result. Though the results are not superior to some of the state-of-the-art methods, the mechanism is innovative and worth using in many applications. It should be pointed out that the proposed method aims at producing pseudo-color fusion image, its visual effect cannot be assessed by its luminance component. From this point of view, the results of Fig. 6 are more reasonable than Fig. 7. The quantitative objective assessment methods assess the quality of the luminance component and chroma component. The results of chroma component evaluation are consistent with the human visual system. Due to the limitation of assessment methods, the assessment results are not precise in evaluating the chroma component of fused images. The visual effect of the pseudo-color fused images generated by our method can give us more comprehensive description, but the chroma information transmitting mechanism and construction method of fused images need further research. The combination of biologically-inspired method and

the traditional signal-decomposition method is our future emphasis content for study and application.

Acknowledgments

References

1. A. Bera, D. Bhattacharjee and M. Nasipuri, Fusion-based hand geometry recognition using Dempster–Shafer theory, *Int. J. Pattern Recognit. Artif. Intell.* **29**(5) (2015) 1556005.
2. Y. Bin, Y. Chao and H. Guoyu, Efficient image fusion with approximate sparse representation, *Int. J. Wavelets Multiresolution Inf. Process.* **14**(4) (2016) 1650024.
3. P. Burt, The pyramid as structure for efficient computation, in *Multiresolution Image Processing and Analysis* (Springer-Verlag, New York, 1984), pp. 6–35.
4. G. Farias, C. S. Martin and F. Gallardo, Study of local matching-based facial recognition methods using thermal infrared imagery Gabriel Hermosilla, *Int. J. Pattern Recognit. Artif. Intell.* **29**(8) (2015) 1556012.
5. D. Gambhir and M. Manchanda, A novel fusion rule for medical image fusion in complex wavelet transform domain, *Int. J. Image Graph.* **16**(4) (2016) 1650022.
6. S. Grossberg and N. A. Schmajuk, Neural dynamics of attentionally modulated pavlovian conditioning: Conditioned reinforcement, inhibition, and opponent processing, *Psychobiol.* **15**(3) (1987) 195–240.
7. J. Kim and S. Lee, Fully deep blind image quality predictor, *IEEE J. Sel. Topics Signal Process.* **11**(1) (2017) 206–220.
8. A. J. King, The integration of visual and auditory spatial information in the brain, in *Higher Order Sensory Processing*, ed. D. M. Guthrie (The University Press, Manchester, 1990), pp. 75–113.
9. E. H. Land, Color vision and the natural image. Part I, *Proc. Natl. Acad. Sci.* **45** (1959) 115–129.
10. E. H. Land, Experiments in color vision, *Sci. Am.* **200** (1959) 84–99.
11. E. H. Land, Recent advances in retinex theory and some implications for cortical computations: Color vision and the natural image, *Proc. Natl. Acad. Sci. USA* **80** (1983) 5163–5169.
12. D. Lee and K. N. Plataniotis, Toward a no-reference image quality assessment using statistics of perceptual color descriptors, *IEEE Trans. Image Process.* **25**(8) (2016) 3875–3889.
13. H. B. Mitchell, *Image Fusion Theories, Techniques and Applications* (Springer-Verlag, Berlin Heidelberg, 2010).
14. E. A. Newman and P. H. Hartline, Integration of visual and infrared information in bimodal neurons of the rattlesnake optic tectum, *Science* **213** (1981) 789–791.
15. P. Scheffel, R. Fish, R. Knobler and T. Plummer, Distributed multi-sensor fusion, multisensor, multisource information fusion: Architectures, algorithms, and applications 2008, in *Proc. SPIE* (Orlando, Florida, 2008), Vol. 6974, pp. 69740P-1-9.
16. A. Seal, D. Bhattacharjee, M. Nasipuri, C. Gonzalo-Martin and E. Menasalvas, Fusion of visible and thermal images using a directed search method for face recognition, *Int. J. Pattern Recognit. Artif. Intell.* **31**(4) (2017) 1756005.

17. V. P. Shah and N. H. Younan, An efficient pan-shapening method via a combined adaptive PCA approach and contourlets, *IEEE Trans. Geosci. Remote Sens.* **46**(5) (2008) 1323–1335.

18. J. Wang, J. Liang, H. Hu, Y. Li and B. Feng, Performance evaluation of infrared and visible image fusion algorithms for face recognition, in *Proc. Int. Conf. Intelligent Systems and Knowledge Engineering* (ISKE, 2007), pp. 1–8.

19. A. M. Waxman *et al.*, Information fusion for image analysis: Geospatial foundations for higher-level fusion, in *Proc. Fifth Int. Conf. Information Fusion*, Vol. 1 (2002), pp. 562–569.

20. A. M. Waxman *et al.*, Multisensor image fusion & mining: From neural systems to COTS software, *Int. Conf. Integration of Knowledge Intensive Multi-Agent Systems* (2003), pp. 355–362.

21. A. M. Waxman *et al.* Solid-state color night vision: Fusion of low-light visible and thermal infrared imagery, *Linc. Lab. J.* **11**(1) (1998) 41–60.

22. A. M. Waxman, A. Gove and D. A. Fay, Night vision: Opponent processing in the fusion of visible and IR imagery, *Neural Netw.* **10**(1) (1997) 1–6.

23. A. M. Waxman, M. C. Seibert, A. Gove and D. A. Fay, Neural processing of targets in visible, multispectral IR and SAR imagery, *Neural Netw.* **8** (1995) 1029–1051.

24. C. Xydaes and V. Petrovi, Objective image fusion performance measure, *Electron. Lett.* **36**(4) (2000) 308–309.

25. J.-L. Wu and X.-L. Tian, Image fusion for mars data using mix of robust PCA, *Int. J. Pattern Recognit. Artif. Intell.* **31**(1) (2017) 1754002.
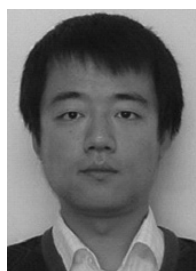
Yuqing Wang received his B.S. and M.S. degrees, both in Electrical Engineering, from Jilin University, Changchun, China, in 2002 and 2005, respectively. In 2008, he received his Ph.D. in Optical Engineering from Changchun Institute of Optics, Fine Mechanics and Physics (CIOMP), Chinese Academy of Sciences, Changchun, China. From August 2008 to August 2010, he was at CIOMP as a post-doctoral fellow in Mechanical and Electronic Engineering. He is currently an Associate Professor at this institute. His research interests include image fusion, image quality assessment, small target tracking and image enhancing.

Yong Wang received her B.S. degree in Communication Engineering from Jilin University, Changchun, China, and her Ph.D. in Mechanical Electronic Engineering from Changchun Institute of Optics, Fine Mechanics and Physics (CIOMP), Chinese Academy of Sciences, China, in 2004 and 2010, respectively. She is currently an Associate Professor with the Department of Communication Engineering, Jilin University. Her interests include image quality assessment, image fusion, Joint Transform Correlator and target tracking.